Eur Biophys J (1997) 25: 463–469

ARTICLE

A. J. Beavil · R. L. Beavil

Automated hydrodynamic modelling of a complex between a human IgE fragment (Fcε3–4) and the IgE high affinity receptor FcεRI α-chain

Received: 31 July 1996 / Accepted: 1 December 1996

Abstract The binding of IgE to its high affinity receptor FcεRI plays an important role in the allergic response. The interaction between soluble FcεRIα-chain (sFcεRIα) and Fcε3–4, a fragment of IgE consisting of the Cε3 and Cε4 heavy chain constant domains, has been studied using analytical ultracentrifugation (Keown et al. this volume). Here we describe the development of a simple automated hydrodynamic modelling technique and its application to this interaction. This procedure utilises sphere models of the two molecules and performs an automated systematic translational search of sFcεRIα relative to Fcε3–4. The result of this is the generation of 40,359 individual models of how the receptor can be placed relative to Fcε3–4. These are then assessed for consistency by comparing the sedimentation coefficients generated for the models to the experimentally determined sedimentation coefficients, and are displayed graphically to show allowed and disallowed complexes. From this analysis, it is clear that the complex between sFcεRIα and Fcε3–4 is compact, with the most elongated models being excluded. In addition, sFcεRIα appears not to interact with the C-terminal end of Fcε3–4, and probably binds either to the sides or face, observations which are consistent with other experimental data on the FcεRIα/IgE interaction. Automated hydrodynamic modelling also has the potential to be used for other interactions, providing a simple way of looking at a large number of models, and making rigorous studies of interacting components more feasible.

Key words FcεRI · IgE · Analytical ultracentrifuge · Automated hydrodynamic modelling

A. J. Beavil (✉) · R. L. Beavil
The Randall Institute, King's College London, 26–29 Drury Lane, London WC2B 5RL, United Kingdom (Fax: 0171 497 9078)

Introduction

The affinity of IgE for its high affinity cell-surface receptor FcεRI ($K_a = 10^{10}$ M^{-1}) is more than an order of magnitude greater than that for antibodies of any other class with any known Fc receptor (Ravetch and Kinet 1991). The stability of the interaction may be inseparable from the role of IgE in immediate hypersensitivity reactions and fortuitously makes it amenable to study by hydrodynamic methods. IgE binds through its Fc portion to FcεRI on mast cells and basophils, and when this receptor-bound IgE is cross-linked by multivalent antigen, it results in the release of inflammatory mediators, and immediate type I hypersensitivity. Consequently, studies on the IgE-receptor complex yield information important for developing strategies to combat allergic reactions, such as peptides which inhibit IgE-FcεRI binding specifically (McDonnell et al. 1996).

FcεRI is made up of four chains (α, β, γ2), but the extracellular portion of the α-chain, comprising two single immunoglobulin-like domains, is sufficient to generate full binding affinity (Hakimi et al. 1990; Blank et al. 1991). The binding sites have been mapped to Cε3 in the IgE-Fc (Helm et al. 1988; Nissim and Eshhar 1992; Basu et al. 1993; reviewed in Sutton and Gould 1993 and Beavil et al. 1993), and to the second, membrane-proximal immunoglobulin-like domain, α2, in the α-chain (Nissim and Eshhar 1992; Basu et al. 1993; Robertson 1993; Scarselli et al. 1993; reviewed in Hulett and Hogarth 1994).

Although the binding sites in IgE and FcεRI are roughly defined, little is known about the arrangement of the two ligands in the complex. Using recombinant IgE-Fc and a soluble recombinant fragment of FcεRI α-chain (sFcεRIα) containing the two immunoglobulin-like domains, we have, in a previous study, been able to determine both the stoichiometry of the complex and its approximate shape in free solution (Keown et al. 1995). The stoichiometry of binding is 1:1, and it appears that possible modes of binding are restricted to those in which there is considerable overlap of the immunoglobulin domains. The hydrodynamic modelling carried out in that study was relatively

crude, since only 20–30 models representing limiting forms of the complex were examined. In addition, the bend in IgE-Fc was not well characterised, which constrained the interpretation of the models. Even now, the range of possible modes of bending envisaged for IgE-Fc (Beavil et al. 1995) would lead to an impossibly large number of models of the complex. Hence, we have studied the complex formed between sFcεRIα and a smaller recombinant fragment of IgE (Fcε3–4) which contains only the Cε3 and Cε4 domains and is therefore unlikely to be bent. We have also attempted to refine the hydrodynamic model of the Fcε3–4/sFcεRIα complex by introducing an automatic procedure to generate many thousands of models representing different orientations of the complex. This is analogous to the AUTOSCT procedure for modelling small angle scattering data, previously described in Beavil et al. (1995).

Materials and methods

Sedimentation velocity studies

Protein samples were a kind gift of M. Keown (Keown et al., this volume). Sedimentation velocity experiments were performed at 20.0 °C using the Beckman Optima XL-A centrifuge with an An60 Ti rotor at speeds from 40,000 rpm to 50,000 rpm for both Fcε3–4 and its complex with sFcεRIα. The sedimentation coefficient for sFcεRIα was previously determined (Keown et al. 1995). Protein concentrations corresponded to A_{280} in the range 0.5–0.8. Data were acquired as absorbance measurements at a wavelength of 280 nm and a radial spacing of 0.003 cm and analysed with the program XLAVEL (Beckman) to yield the uncorrected sedimentation coefficient. Data were collected at three concentrations, s was extrapolated to zero concentration, and then corrected to obtain $s^0_{20,w}$ as previously described for IgE-Fc (Keown et al. 1995).

Determination of hydrodynamic parameters

The partial specific volume, relative molecular mass and volume of recombinant IgE-Fc and sFcεRIα were calculated from the amino acid compositions, together with estimated carbohydrate contents (Perkins 1986), and are shown in Table 1. The sedimentation coefficients for the two components separate and when complexed were determined as described for IgE-Fc and sFcεRI-α (Keown et al. 1995).

Table 1 Composition data for Fcε3–4, sFcεRIα and their complex

	M_r	$\bar{v}$ ($cm^3\,g^{-1}$)	Dry volume (nm^3)	Dry model volume (nm^3)
Fcε3–4	52 772	0.728	66.9	63.6
sFcεRIα	33 782	0.698	40.5	36.6
Complex	86 554	0.716	107.4	103.6

Generation of sphere models of Fcε3–4, sFcεRIα and their complex

To calculate simulated hydrodynamic parameters, models made from small non-overlapping spheres were generated. These do not represent chemically defined subunits but are used only to approximate a simple structure. Crystal co-ordinates of either the whole protein structure or a single domain can be converted into a sphere model. In this case, model calculations of the sedimentation coefficients were based on the IgE-Fc models of Padlan and Davies (1986), and Helm et al. (1991), and on a model of sFcεRIα based on the crystal structure of CD2 (McDonnell et al. 1996; Beavil et al. 1993; Jones et al. 1992). Whilst a model of sFcεRIα by Padlan and Helm has been published (1992), it is currently unavailable in the Brookhaven Protein Data Bank, but it would not be expected to yield a significantly different sedimentation coefficient, as the methods used here are only sensitive to gross configuration. Unlike the case of IgE-Fc, the possibility that Fcε3–4 could exhibit bending within the Cε2–Cε3 linker region does not have to be investigated, as the Cε2 domains are not present, and this simplifies the situation considerably. Carbohydrate chains were modelled on those found in the human Fc crystal structure (Deisenhofer 1981). These were attached to the putative carbohydrate sites on the proteins using Insight II molecular graphics software (Biosym Technologies, Inc.).

For calculations of the hydrodynamic models, the molecular models were first converted into spheres using a program BRKTOS in which the model was placed in a three dimensional grid of cubes (Smith et al. 1990; Perkins et al. 1993). The cubes were included as the building blocks of the hydrodynamic model if they contained at least one α-carbon atom. The dimensions of the cubes were optimised such that the total volume of the cubes equalled that of the dry protein volume calculated from the composition above (66.9 nm^3 and 40.5 nm^3 for Fcε3–4 and sFcεRIα, respectively). The volumes were then increased to allow for a hydration shell, assumed to comprise 0.3 g of water/g glycoprotein and an electrostricted volume of 0.0245 nm^3 per bound water molecule (Perkins 1986; Smith et al. 1990; Perkins et al. 1993). The resulting models were assigned co-ordinates to produce the final hydrodynamic models based on non-overlapping spheres placed at the centre of each cube, which now had sides of 0.707 nm. Hydrodynamic calculations were performed by the modified Oseen tensor procedure using the program GENDIA (Garcia de la Torre 1977a, b, 1989). This method of generating sphere models is very crude but it has an interesting advantage over other methods in so far as it allows one to detect overlap between the two components of the complex by analysing the number of spheres or volume of the final model of the complex. We have also found that as expected, it is the volume excluded by the surface of the model which is important to the calculation of the frictional coefficients and not the volume of the spheres themselves.

Axis definitions for the components of the complex

The origin of Fcε3–4 was set as a pseudoatom defined as the centre of mass of the molecule. Its x-axis was defined both by this pseudoatom and a second pseudoatom at the geometrical centre of residue 333 from the A and B chain, and the x-y plane was defined by the addition of a pseudoatom at the centre of mass of the A chain. The origin of sFcεRIα was initially set as a pseudoatom defined as the centre of mass of residues 100–176; its x-axis was defined both by this pseudoatom and a second pseudoatom at the centre of mass of residues 2–99; the x-y plane was defined by the addition of a pseudoatom at the centre of mass of the whole molecule. The origin was then translated to the centre of mass of the whole molecule (see Fig. 1).

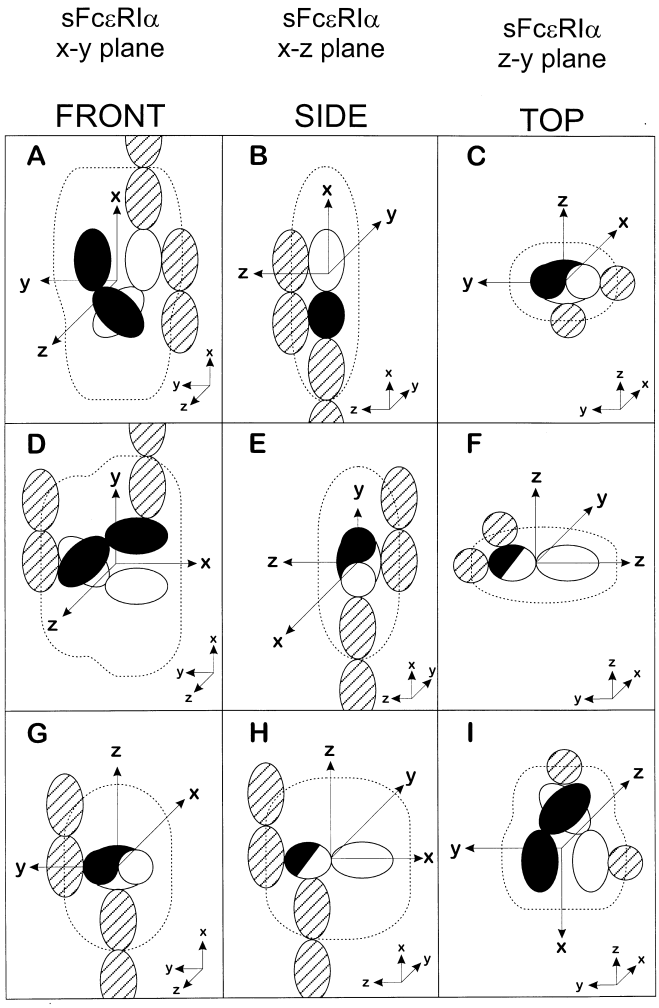

Fig. 1A–I Schematic diagram of the Fcε3–4/sFcεRIα complex models. The two chains of Fcε3–4 are shown *shaded* and *open*, and sFcεRIα is *hatched*, with two of its many possible positions depicted in each panel. Models are viewed projected onto orthogonal planes defined by the axes of sFcεRIα. The x–y plane is the front view, x–z is the side view and z–y the top view. **A–C** represent Fcε3–4 in the 'vertical' orientation, **D–F** the 'horizontal', and **G–I** the 'front-back' orientation. The Fcε3–4 axes are shown for each view together with the corresponding axes of sFcεRIα. The *dotted outline* shows the path traced out by the centre of mass of sFcεRIα for a non-overlapping complex

Table 2 Search ranges and number of models associated with each of the three translational searches are defined. The translations were performed in 0.5 nm steps

	x range (nm)	y range (nm)	z range (nm)	Total models
Vertical	–9.0 to +9.0	–5.0 to +5.0	–4.0 to +4.0	13 209
Horizontal	–8.0 to +8.0	–6.0 to +6.0	–4.0 to +4.0	14 025
Front-back	–6.0 to +6.0	–5.0 to +5.0	–6.0 to +6.0	13 125

Systematic translational searches

A series of INSIGHT II (Biosym Technologies, Inc.) macros were developed, based on the AUTOSCT package (Beavil et al. 1995), and these were used to explore three degrees of translational freedom between the two elements of the complex. sFcεRIα was driven along its axes in a concerted stepwise manner by a series of nested loops within the macro scripts to generate many thousands of models. Taking the origin as when both centres of mass are superimposed, sFcεRIα was translated in steps of 0.5 nm along its own x, y and z axes such that it traced out a three-dimensional grid (search grid), the dimensions of which were varied according to the orientation of Fcε3–4. Fcε3–4 was placed in one of three orientations. The first (referred to as vertical) consists of both sFcεRIα and Fcε3–4 sharing identically aligned long (x) axes. The second (horizontal) has Fcε3–4 lying at 90° following a +90° rotation about its z axis. The third (front-back) has a rotation of +90° about the y axis. The models are shown in Fig. 1, and Table 2 shows the translational range and the number of models associated with each of the three translational searches.

Results

The sphere models generated are an accurate representation of the complex

The sphere models generated for Fcε3–4 and sFcεRIα were used to calculate sedimentation coefficients. Both of these were within 0.1 S of the experimental values (Table 3), indicating the individual models forFcε3–4 and sFcεRIα were accurate representations of each protein. The models for the complexes were examined and it was found that in a non-overlapping complex the volume varied (Table 1), but was never underestimated by more than

Table 3 Sedimentation coefficients determined experimentally or calculated from models of Fcε3–4, sFcεRIα and their complex

	Experimental $s^0_{20,w}$ (S)	Calculated $s^0_{20,w}$ (S)
Fcε3–4	3.77 ± 0.05	3.85
sFcεRIα	2.80 ± 0.05	2.73
Complex	4.95 ± 0.05	3.4 to 6.4

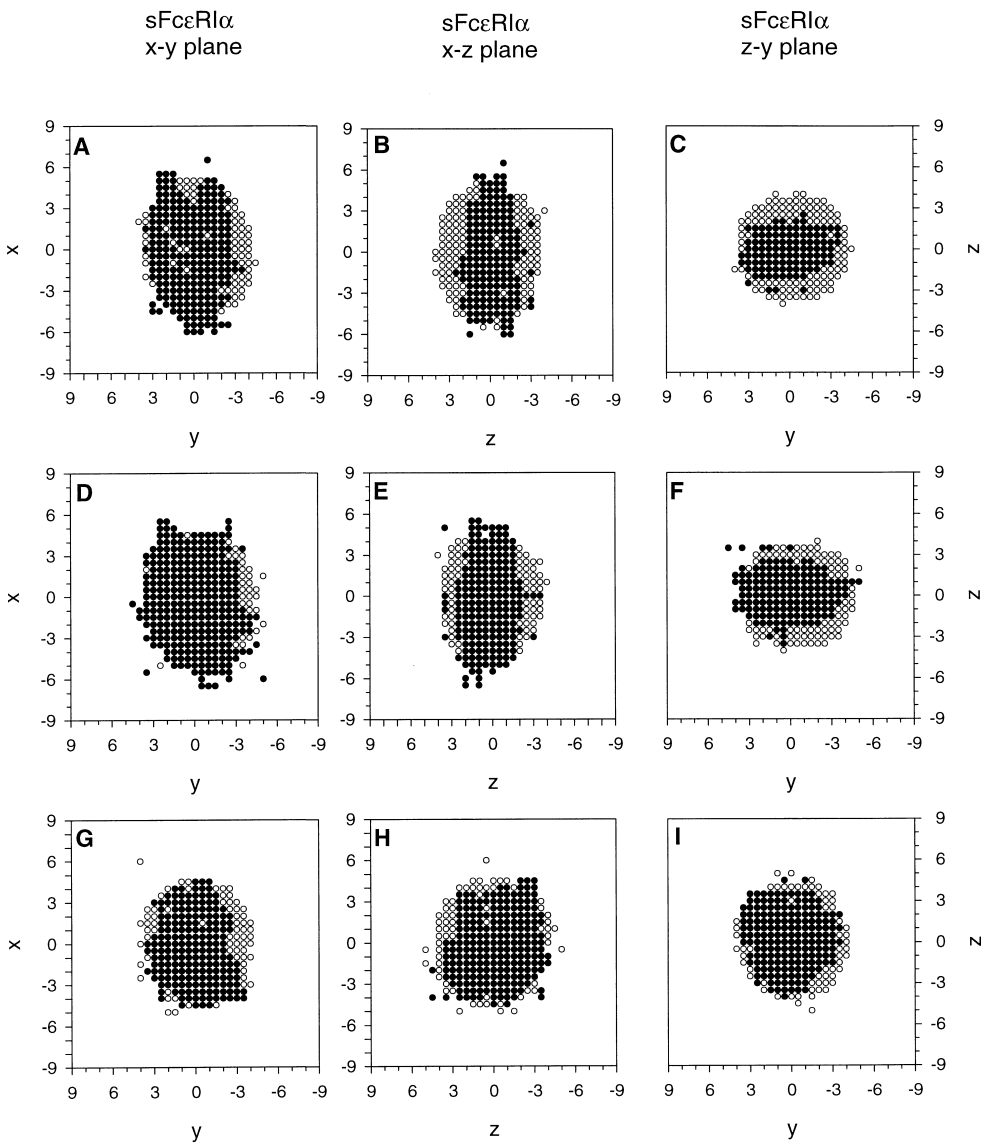

Fig. 2A–I Scatter plots of the Fcε3–4/sFcεRIα complex models. Models are viewed projected onto orthogonal planes defined by the axes of sFcεRIα (as in Fig. 1) with dimensions of nm. The *solid dots* represent the models with between 360–370 spheres and essentially define the shape of Fcε3–4. The *hollow dots* represent models with a calculated $s^0_{20,w}$ within ±0.1S of the experimentally observed value, and define which surfaces of Fcε3–4 may be occupied by sFcεRIα within the complex. The interpretation of these data, in terms of which faces of Fcε3–4 are available for binding sFcεRIα, is given in Table 4

3.5%, depending upon the orientation and this has no significant effect on the calculated frictional coefficients.

Visual interpretation of the data

Table 3 shows the experimentally derived sedimentation coefficients for the complex and its two components together with the corresponding results from the models. Interpreting the data from 40,359 models is far from a trivial task. We have chosen to display the data in the form of a scatter plot (Fig. 2) which shows orthogonal views of the complex projected onto three planes from each of the three possible orientations for Fcε3–4, namely, (in terms of the axes of sFcεRIα which remain invariant throughout), the x-y plane (front view), the x-z plane (side view) and the z-y plane (top view). Figure 1 shows schematically the orientation of the two components of the complex in each of the panels in Fig. 2. In looking at the data, there are several things which must be considered. To a first approximation, the filled circles define the outline of the Fcε3–4 and the open circles delimit the regions of the surface that sFcεRIα may inhabit. The filled circles represent models with between 360 and 370 spheres inclusive and the open circles represent models with more than 370 spheres (i.e., minimal overlap) but with a sedimentation coefficient within a fixed range of the experimental value for the complex of ±0.1S. If no overlap occurs between the two component models when they are in the search grid before the spheres are assigned, 401 spheres should appear in the sphere model although spurious effects related to the precise orientation of the molecular model within the search grid give rise to small fluctuations in the number of spheres. Overlap between the models results in a reduction of the number of spheres. We have used a loss of around 5% of the spheres as indicating the beginning of overlap i.e. 380

spheres or less. The decision to represent Fcε3–4 by those models with between 360 and 370 spheres is an arbitrary one. When set at 370, the representations give a more interpretable outline to Fcε3–4.

Whilst considering the shape of Fcε3–4, it should be noted that rather than define the surface of Fcε3–4, the filled circles actually trace out the centre of mass of sFcεRIα. The consequence of this is that if sFcεRIα approaches Fcε3–4 'end on', it will begin to overlap further from the surface that if it approaches 'side on' (one domain length as opposed to half a domain width). As an example, consider panels C and G which from the schematic diagram would be expected to have the same shape, but look quite different as sphere models. The dotted lines in the schematic diagram show the expected shape distortion for each orientation. In addition, the representations shown in Fig. 2 are asymmetrical. This is a reflection of the fact that the sFcεRIα model used is asymmetric, having a bend between the two immunoglobulin domains, and also having an uneven glycosylation profile (McDonnell et al. 1996).

Comparison with experimental data

Table 4 shows a summary of the each of the panels in Fig. 2. We have considered the possibility of sFcεRIα approaching the flat face, sides and ends of Fcε3–4 in all of the possible orientations, and we have indicated whether each position is possible, marginal or excluded. In each case, one of the approaches does not apply, as the data in every panel represents the movement of sFcεRIα using only two of the axes, to enable two-dimensional representation of the data. There is also some overlap between models, as some of the extreme configurations occur in more than one panel, but this serves to strengthen any conclusions drawn. In summary, if the long axis of sFcεRIα is parallel to the long axis of Fcε3–4, i.e. vertical (panels A, B and C), it is clear that the sFcεRIα can sit on the flat face or sides of Fcε3–4, but not on the bottom, and probably not on the top. If, however, the long axis of sFcεRIα is perpendicular to the long axis of Fcε3–4 (horizontal) as shown in panels D, E and F, sFcεRIα can occupy the flat face, and possibly the top, but the bottom and sides are excluded. The last set of models, G, H and I, with sFcεRIα end on to the flat face of Fcε3–4 (front-back), indicate that sFcεRIα in this orientation can occupy the flat face, and possibly the sides and ends. From this information, it is clear that only the more compact models are compatible with the experimental data, and elongated models are ruled out.

Table 4 Interpretation of the data shown in Fig. 2, indicating which faces of Fcε3–4 are available for binding sFcεRIα. An indication of the level of confidence in the prediction is given by either Yes, No or Marginal, and where possible to which end of Fcε3–4 the prediction belongs

	x−y plane	x−z plane	z−y plane
Vertical (A, B, C)	Flat: N/A Sides: Yes Ends: Marginal (Top)	Flat: Yes Sides: N/A Ends: No	Flat: Yes Sides: Marginal Ends: N/A
Horizontal (D, E, F)	Flat: N/A Sides: No Ends: Marginal (Top)	Flat: Yes Sides: No Ends: N/A	Flat: Yes Sides: N/A Ends: Marginal (Top)
Front-back (G, H, I)	Flat: Marginal Sides: Yes Ends: N/A	Flat: Marginal Sides: N/A Ends: Yes	Flat: N/A Sides: Yes Ends: Marginal

Discussion

The aim of this study was to analyse the Fcε3–4/sFcεRIα complex more thoroughly than had previously been attempted. It has led to the creation of an automated method for easily generating large numbers of models, in this case 40,359, and comparing them all to experimentally determined sedimentation coefficients. Despite any possible objections based on uncertainty in the quantity of hydration associated with the hydrodynamic models, the precision associated with the agreement of calculated sedimentation coefficients with experimental data has been calibrated by Perkins (1993) and shown to be on average close to ±0.1S. The sedimentation coefficients we have calculated for Fcε3–4 and sFcεRIα alone fall within this range (Table 3). We have used this as a cut off value to analyse the models we have produced, although less restrictive cut off values up to ±0.3S yield similar results (data not shown).

The results obtained are more rigorous than those presented in Keown et al. 1995 for the IgE-Fc/sFcεRIα complex, and although it is impossible to define the IgE/sFcεRIα interaction precisely, the results presented in Fig. 2 and Table 4 indicate that many binding configurations can be ruled out. It appears that the interaction between Fcε3–4 and sFcεRIα is fairly compact, as elongated models are not compatible with the experimental data. It also suggests that sFcεRIα is unlikely to be interacting with the bottom of Fcε3–4, and probably lies either along the sides or on the flat face. This is consistent with other experimental data on sFcεRIα binding to IgE and its recombinant fragments. It is known that domain 2 of sFcεRIα (Nissim and Eshhar 1992; Basu et al. 1993; Robertson 1993; Scarselli et al. 1993; reviewed in Hulett and Hogarth 1994) binds to the Cε3 domains of IgE (Helm et al. 1988; Nissim and Eshhar 1992; Basu et al. 1993; reviewed in Sutton and Gould 1993 and Beavil et al. 1993), which confirms the fact that sFcεRIα cannot lie along the bottom of Fcε3–4. As domain 2 of sFcεRIα is the membrane-proximal domain in the native protein, it is also unlikely that it is able to bind 'end-on' to IgE: this is confirmed by the fact that models where sFcεRIα interacts 'end-on' with the Fcε3–4 are not compatible with the experimentally determined sedimentation coefficients. This study could not determine whether binding was on the sides or face of Fcε3–4, however.

The calculations performed in this study took the equivalent of nine days of CPU time on 100 MHz Silicon Graphics Indy R4000SC UNIX workstations. In fact, the method is very amenable to parallel processing techniques, and the whole exercise was completed over a single weekend, once set up, by splitting the tanks and running it concurrently on three identical workstations. The hydrodynamic calculations were performed using GENDIA rather than HYDRO (Garcia de la Torre et al. 1994) because of the relative difference in speed, which is almost an order of magnitude. However, development of a small dedicated program for manipulating the molecular models, rather than the use of Insight II, combined with a tighter integration of the other functions could easily generate a speed increase sufficient to make the use of the more rigorous program HYDRO a practical proposition. The use of HYDRO would also enable a number of additional hydrodynamic parameters such as intrinsic viscosity, translational diffusion coefficients and rotational relaxation times to be included as additional constraining factors. Any other constraints to the model are easily incorporated in the calculations, and this may include data from a wide variety of sources such as X-ray or neutron scattering studies (for example, see Beavil et al. 1995). This kind of automated modelling is feasible for anyone with an entry-level workstation, and could be further developed, for example using Monte Carlo methods. It should certainly be considered by anyone studying a reasonably elongated high affinity complex.

Because this method uses models based on the known structure of domains, it is more specific than other methods which model proteins as simple geometric shapes. Whilst it is still not possible to analyse the experimental data so as to arrive at a unique structure which fits the data, given a range of models, it is possible to filter out implausible structures. The more filters that can be applied to the agreement between the models and the experimental data, the more confidence one can have in the limits that are defined by the modelling procedure. In many applications it should be possible to arrive at a very limited range of models which fit both the experimental data and the constraints known to apply to the structure.

The automated hydrodynamic modelling method described here clearly has the potential to define the limits of interactions between the components of a complex in a far more thorough way than has been possible in the past. In the future, it will be essential to undertake a rigorous examination and calibration of the limits of the calculations. This technique has the benefits of being automatic, once the axes of the two components have been defined, and enables all possible orientations of the components relative to one another to be investigated. Conventional modelling techniques, where each complex is built by hand do not feasibly allow such a thorough study to be carried out, so the application of this technique represents a significant advance in the study of complex formation using hydrodynamic methods.

Acknowledgements We thank M. B. Keown for providing the protein samples and Dr. R. Ghirlando for assistance with the ultracentrifugation. Our work in this field has been greatly assisted by the support and interest of Dr. S. J. Perkins, and by access to computer software developed by him. We thank Dr. B. J. Sutton and Prof. H. J. Gould for supporting our interest in this work. We gratefully acknowledge the financial support of the Medical Research Council and the Wellcome Trust.

References

Basu M, Hakimi J, Dharm E, Kondas JA, Tsien WH, Pilson RS, Lin P, Gilfillan A, Haring P, Braswell EH, Nettleton MY, Kochan JP (1993) Purification and characterisation of human IgE-Fc fragments that bind to the human high affinity IgE receptor. J Biol Chem 268:13118–13127

Beavil AJ, Beavil RL, Chan CMW, Cook JPD, Gould HJ, Henry AJ, Owens RJ, Shi J, Sutton BJ, Young RJ (1993) Structural basis of the IgE-FcεRI interaction. Biochem Soc Trans 21:968–972

Beavil AJ, Young RJ, Sutton BJ, Perkins SJ (1995) Bent domain structure of recombinant human IgE-Fc in solution by X-ray and neutron scattering in conjunction with an automated curve fitting procedure. Biochemistry 34:14449–14461

Blank U, Ra CS, Kinet J-P (1991) Characterisation of truncated α-chain products from human, rat and mouse high affinity receptor for immunoglobulin E. J Biol Chem 266:2639–2646

Deisenhofer J (1981) Crystallographic refinement and atomic models of a human Fc fragment and its complex with fragment B of protein A from *Staphylococcus aureus* at 2.9- and 2.8-Å resolution. Biochemistry 20:2361–2370

Garcia de la Torre J, Bloomfield VA (1977a) Hydrodynamic properties of macromolecular complexes. I. Translation. Biopolymers 16:1747–1761

Garcia de la Torre J, Bloomfield VA (1977b) Hydrodynamics of macromolecular complexes. III. Bacterial viruses. Biopolymers 16: 1779–1793

Garcia de la Torre J (1989) In: Harding SE, Rowe AJ (ed) Dynamic properties of biomolecular assemblies. Royal Society of Chemistry, Cambridge, pp 3–31

Garcia de la Torre J, Navarro S, Lopez Martinez MC, Diaz FG, Lopez Cascales (1994) HYDRO: A computer program for the prediction of hydrodynamic properties of macromolecules. Biophysical J 67:530–531

Hakimi J, Seals C, Kondas JA, Pettine L, Danho W, Kochan J (1990) The α subunit of the human IgE receptor (FcεRI) is sufficient for high affinity IgE binding. J Biol Chem 265:22079–22081

Helm B, Marsh P, Vercelli D, Padlan E, Gould H, Geha RS (1988) The mast cell binding site on human IgE. Nature 331:180–183

Helm BA, Ling Y, Teale C, Padlan EA, Bruggemann M (1991) The nature of the importance of the inter-ε chain disulphide bonds in human IgE. Eur J Immunol 21:1543–1548

Hulett MD, Hogarth PM (1994) Molecular basis of Fc receptor function. Adv Immunol 57:1–127

Jones EY, Davis SJ, Williams AF, Harlos K, Stuart DI (1992) Crystal-structure at 2.8-angstrom resolution of a soluble form of the cell-adhesion molecule CD2. Nature 360:232–239

Keown MB, Ghirlando R, Yong RJ, Beavil AJ, Owens RJ, Perkins SJ, Sutton BJ, Gould HJ (1995) Hydrodynamic studies of a complex between the Fc fragment of human IgE and a soluble fragment of the FcεRI α-chain. Proc Natl Acad Sci USA 92:1841–1845

McDonnell JM, Beavil AJ, Mackay GA, Jameson BA, Korngold R, Gould HJ, Sutton BJ (1996) Structure based design and characterisation of peptides that inhibit IgE binding to its high affinity receptor. Nature Struct Biol 3:419–426

Nissim A, Eshhar Z (1992) The human mast cell receptor binding site maps to the third constant domain of immunoglobulin E. Mol Immunol 29:1065–1072

Padlan EA, Davies DR (1986) A model of the Fc of Immunoglobulin E. Molec Immunol 23:1063–1075

Padlan EA, Helm BA (1992) A modeling study of the α-subunit of human high-affinity receptor for immunoglobulin E. Receptor 2:129–144

Perkins SJ (1986) Protein volumes and hydration effects – the calculations of partial specific volumes, neutron-scattering matchpoints and 280-nm absorption-coefficients for proteins and glycoproteins from amino-acid sequences. Eur J Biochem 157: 169–180

Perkins SJ, Smith KF, Kilpatrick JM, Volanakis JE, Sim RB (1993) Modelling of the serine-proteinease fold by X-ray and neutron scattering and sedimentation analysis: occurrence of the fold in factor D of the complement system. Biochem J 295:87–99

Ravetch JV, Kinet JP (1991) Fc receptors. Ann Rev Immunol 9:457–492

Robertson MW (1993) Phage and *Escherichia coli* expression of the human high affinity immunoglobulin E receptor α-subunit ectodomain. J Biol Chem 268:12736–12743

Scarselli E, Esposito G, Traboni C (1993) Receptor phage-display of functional domains of the human high affinity IgE receptor on the M13 phage surface. Febs Lett 329:223–226

Smith KF, Harrison RA, Perkins SJ (1990) Structural comparisons of the native and reactive-center-cleaved forms of alpha-1-antitrypsin by neutron-scattering and X-ray-scattering in solution. Biochem J 267:203–212

Sutton BJ, Gould HJ (1993) The human IgE network. Nature 336:421–428